New Type of Dual Solid-State Thermochromism: Modulation of Intramolecular Charge Transfer by Intermolecular $\pi-\pi$ Interactions, Kinetic Trapping of the Aci-Nitro Group, and Reversible Molecular Locking

Panče Naumov,*,† Sang Cheol Lee,‡ Nobuo Ishizawa,§ Young Gyu Jeong,‡ Ihn Hee Chung,‡ and Shunichi Fukuzumi†

Department of Material and Life Science, Graduate School of Engineering, Osaka University, 2-1 Yamada-oka, Suita, Osaka 565-0871, Japan, School of Advanced Materials and Systems Engineering, Kumoh National Institute of Technology, Gumi 730-701, Korea, and Ceramics Research Laboratory, Nagoya Institute of Technology, Tajimi, Gifu 507-0071, Japan

Received: March 19, 2009; Revised Manuscript Received: September 2, 2009

When heated above room temperature, some crystalline polymorphs of the 1,3-bis(hydroxyalkylamino)-4,6-dinitrobenzenes (BDB*n*, $n = 2-5$), bis(hydroxyalkyl) analogues of the intramolecular charge-transfer molecule 1,3-diamino-4,6-dinitrobenzene, exhibit "dual" thermochromism: *gradual* color change from yellow to orange at lower temperatures, and *sharp* color change from orange to red at higher temperatures. These two thermochromic changes are related to different solid-state processes. When allowed to cool to room temperature, the yellow color of the thermochromic molecules with different alkyl length (*n*) is recovered with unexpectedly different kinetics, the order of the respective rate constants ranging from $10^{-7}-10^{-6}$ s^{-1} for BDB2 to about 0.1 s^{-1} in the case of BDB3. The thermochromic mechanism and the reasons behind the different kinetics were clarified on the basis of detailed crystallographic characterization, kinetic thermoanalysis, and spectroscopic study of eight crystalline forms (seven polymorphs and one solvate). It was found that the polymorphism is due to the possibility of "locking" and "unlocking" of the alkyl arms by formation of a strong intramolecular hydrogen bond between the hydroxyl groups at their hydroxyl termini. The locking of BDB2, with shortest alkyl arms, is reversible and it can be controlled thermally; either of the two conformations can be obtained in the solid state by proper thermal treatment. By use of high temperature in situ single crystal X-ray diffraction analysis of BDB3, direct evidence was obtained that the *gradual* thermochromic change is related to increased distance and weakened $\pi-\pi$ interactions between the stacked benzene rings: the lattice expands preferably in the stacking direction, causing enhanced oscillator strength and red shift of the absorption edge of the intramolecular charge transfer transition. The second, *sharp* thermochromic change had been assigned previously to solid−solid phase transition triggered by intramolecular proton transfer of one amino proton to the nitro group, whereupon an aci-nitro form is thermally populated. Contrary to the numerous examples of solid thermochromic molecules based on either pericyclic reactions or keto−enol tautomerism, this system appears to be the first organic thermochromic family where the thermochromic change appears as an effect of intermolecular $\pi-\pi$ interactions *and* thermal intramolecular proton transfer to aromatic nitro group.

Introduction

Organic molecules having large second-order polarizabilities are of importance as nonlinear optical (NLO) materials for photonics applications, including photon-based processing and storage of data. Of particular importance in that respect are two-dimensional octupolar-like charge transfer organic molecules with electron-active substituents in an "X" or a "Λ" arrangement, which exhibit large second-order polarizabilities but are void of the undesired absorption red-shifts observed with other substituent geometries. 1,3-Diamino-4,6-dinitrobenzene (DADNB, Chart 1a) is a prototype X-substituted intramolecular charge transfer (CT) aromatic molecule which has been utilized to study special aspects of the NLO activity such as the anisotropy of the second-order polarizability.[1,2] For instance, the electric-field-induced second harmonic generation and hyper-Rayleigh scattering measurements on its *N*,*N*′-dihexyl derivative showed[2] that contrary to the expected one-dimensional second-order polarizability (predominance of the β_{zzz} component), the second-order polarizability is almost completely due to the off-diagonal components (β_{zyy} and $\beta_{yzy} = \beta_{yyz}$). Being constrained by electron conjugation close to planarity, DADNB is a small and fairly rigid molecule, having both of its amino groups engaged in strong intramolecular hydrogen bonds, and thus less available

CHART 1: Chemical Structures of 1,3-Diamino-4,6-dinitrobenzene (DADNB, a) and 1,3-Bis(hydroxyalkylamino)-4,6-dinitrobenzenes BDB*n*, *n* = 2−5

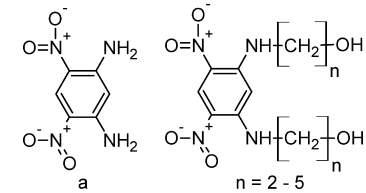

* Corresponding author: telephone, +81-(0)6-6879-4574; fax, +81-(0)6-6879-4726; e-mail, npance@wakate.frc.eng.osaka-u.ac.jp.
† Osaka University.
‡ Kumoh National Institute of Technology.
§ Nagoya Institute of Technology.

10.1021/jp902517x CCC: $40.75
Published on Web 09/28/2009

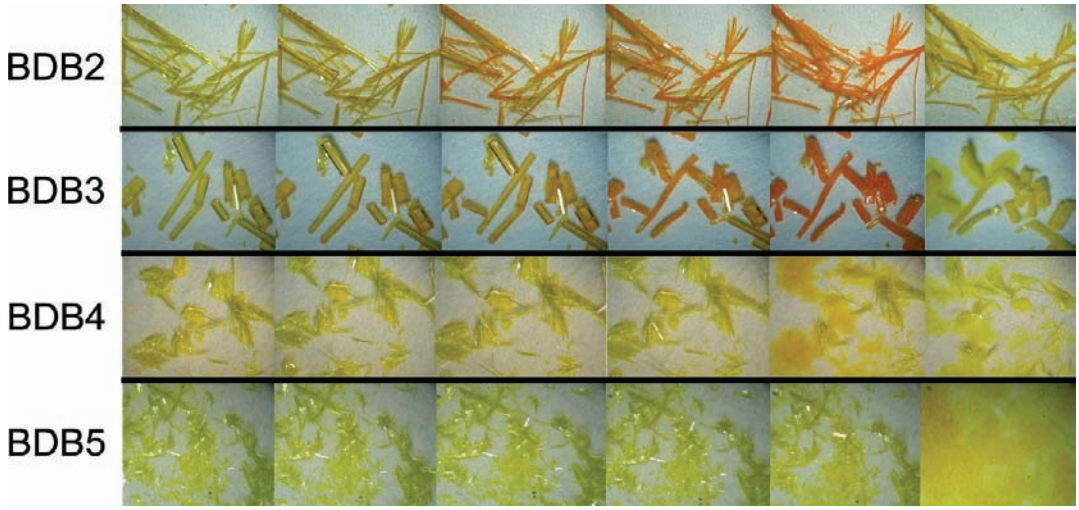

Figure 1. Temperature effects on the appearance of BDB*n* ($n = 2-5$, form A in each case) crystals heated on filter paper. The temperature increases from the left to the right panels. The last images in each row show the respective samples after they were cooled to room temperature. Note that while BDB2 and BDB3 show both gradual (yellow → orange) and sharp (orange → red) phase transitions, BDB4 shows sharp transition to orange-yellow just before the melting. BDB5 melts without any apparent phase transition. As it is shown in the images on the far right, the yellow color of all samples is recovered after they were cooled to room temperature. Apparent is the loss of the translucency and crystal integrity of the single crystals of BDB2, BDB3, and BDB4 after one heating−cooling cycle.

SCHEME 1: General Mechanism of the "Dual" Thermochromic Change of BDB-Type Molecules

BDB(yellow) $\underset{}{\overset{\Delta \text{ gradual}}{\rightleftharpoons}}$ BDB(orange) $\overset{\Delta \text{ sharp}}{\rightleftharpoons}$ BDB(red)

for intermolecular interactions. As a result, DADNB is prone to packing through an assembly of $\pi-\pi$ stacks, which limits the prospects for its utilization as building block for construction of different NLO-active supramolecular structures. Some of us have recently prepared[4] a series of 1,3-bis(hydroxyalkylamino)-4,6-dinitrobenzenes, shown in Chart 1 (BDB*n*, $n = 2-5$), which were designed as semiflexible *N*,*N*′-bis-substituted hydroxyalkyl analogues of DADNB with conformationally supple alkyl arms, containing between two and five carbon atoms, which are terminated by hydroxyl groups. The main advantage of such modified DADNB-type molecules over the DADNB itself is that they provide grounds to explore structure−property relationships in this CT system. Such possibility rests on the combination of alkyl groups with hydrogen bond donor (hydroxyl, amino) and acceptor (nitro) functionalities, which is expected to increase the conformational flexibility while promoting the formation of polymorphs and enhancing the ability for crystallization.

When heated slowly above room temperature (RT), single crystals and microcrystalline powders of some of the BDB*n* compounds exhibit different thermochromic change in two different temperature regimes. Heated crystals of BDB2 and BDB3 initially undergo *gradual* change of their color from yellow to orange-yellow and remain translucent (Figure 1). Further heating of the orange-yellow crystals of BDB2 and BDB3 to high temperature (HT) results in more pronounced, *sharp* change of the orange-yellow color to red or brick-red, whereupon the crystals turn opaque. Thus, BDB2 and BDB3 undergo both gradual and sharp thermochromic changes, that is, they show "dual" thermochromism (Scheme 1). Instead, the crystals of BDB4 do not undergo readily observable gradual color change, but they undergo sharp color change of the yellow crystals to orange. Crystals of BDB5 melt directly, without color change, resulting in a red liquid. The observed thermochromic change of BDB2−4 is reversible, so that on cooling to RT the yellow color is completely recovered, although

SCHEME 2: Schematic Representation of the Nitro−Aci-nitro Tautomerism Suggested for the High Temperature Solid−solid Phase Transition of the BDB*n* Compounds, $n = 2-4$ (BDB5 melts without a preceding solid−solid phase transition)

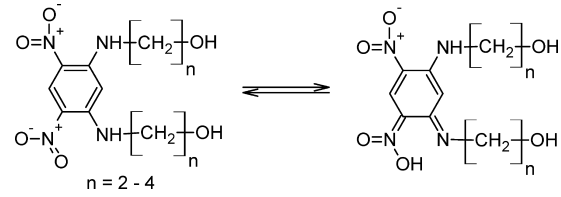

the single crystal specimens remain opaque (Figure 1). The preliminary observations[3,4] of this new solid-state thermochromic system indicated unexpectedly different rates of the color recovery of different BDB*n* compounds: for instance, while the orange-red crystals of the HT form of BDB3 cooled to RT are converted to their yellow form almost instantaneously, the orange color of BDB2 crystals treated in the same way persists for hours before the complete recovery. The structural factors determining such inconsistency have remained unknown because apart from the two polymorphic modifications of BDB2,[3] the crystal structures of the other compounds have yet to be determined. Thus, no quantitative information has so far been reported on the kinetics of the involved processes.

Being interested in structures of unstable and short-lived molecular species,[5] and particularly in reactive intermediates and metastable phases of photochromic and thermochromic compounds, our attention was attracted by the molecular mechanism and the origin of the BDB-type thermochromism, and especially by the factors determining its solid-state kinetics. Of particular significance is the evolution, the structures, and stabilities of the HT forms, which had been spectroscopically identified[3] with the respective monoacidic form of the nitro group −N(O)OH that absorbs around 410−460 nm,[6] termed the aci-nitro group (Scheme 2). The aci-nitro group is an important intermediate in the chemistry of photoactive nitro compounds, such as the bioactive nitroaromatic caged compounds. Although it has been well documented by steady-state and time-resolved spectroscopy as short-lived species in solu-

tions and solids of photoexcited nitroaromatics,[6] except for a single reported case of an aci-nitro group stabilized by intermolecular hydrogen bonding in the crystal of aci-nitrodiphenylmethane at RT,[7] the high energy of the −N(O)OH ground state relative to the nitro form and the flat energy surface associated with the respective proton dissociation have precluded the detailed structural characterization of this important functionality.

Building up on the previous observations,[3,4] we report herein the detailed molecular mechanism of the reversible thermochromic change of the crystalline BDB*n* compounds ($n = 2-5$), and we also unravel the structural factors which affect the stability and the lifetime of their thermochromic forms. The solid-state thermochromism of various organic materials has been often studied by LT single crystal X-ray diffraction. By employing a much less commonly used technique to study organic materials, in situ HT single crystal X-ray diffraction, in combination with kinetic thermoanalytical measurements, we obtained direct experimental evidence that the gradual and sharp thermochromic changes of BDB*n* are based upon substantially different molecular mechanisms. The synergetic effect of the strong intramolecular hydrogen bonding and substituent electronic effects is particularly effective in the structure of BDB2, which results in notable extension of the lifetime of its HT form in the solid state.

2. Experimental and Theoretical Details

2.1. Synthesis and Polymorph Screening. Gram-scale amounts of crystalline BDB*n* were synthesized by reaction of 2,6-dichloro-3,5-dinitrobenzene with a series of aliphatic amino alcohols,[3,4] and were extensively screened for polymorphs by slow evaporation from various solvents at RT and at 283 K. Depending on the solvent, oftentimes concomitant polymorphs were obtained, and occasionally the same polymorph crystallized as several different habits. The structure identity of all crystal habits was checked individually, by comparing the unit cell parameters determined by single crystal X-ray diffraction. In the case of BDB2, three polymorphs (A, B, and D) of four crystal habits were prepared: form A was obtained as acicular (ACN, MeOH, THF), prismatic (ACN, EtOH, EtOAc) and large orange block (THF) crystals, form B crystallized as rhomboidal or trapezoid dark yellow crystals (MeOH, ACN, EtOAc, THF), and form D was obtained as very thin, brittle, platy yellow crystals (EtOAc, THF, ACN). BDB3 afforded needle/stellate/reticular crystals (EtOH, MeOH, THF, EtOAc), prismatic crystals (EtOH, CH_2Cl_2, EtOAc, ACN, MeOH), or platy crystals (CH_2Cl_2), all of which have identical structure. For BDB4, form A was obtained as long prismatic crystals (EtOH at RT), fine needles (EtOH at 283 K), and reticular crystals (acetone), whereas form B crystallized as very long and thin prisms (EtOAc). BDB5 crystallizes as long prismatic triclinic crystals of form A (EtOH). The benzene solvate of BDB5 (form B) was obtained as very thin, elastic yellow orthorhombic plates by slow evaporation of saturated benzene solutions. When exposed to air, the crystals of form B BDB5 gradually turn opaque and loose crystallinity in less than an hour, but they are stable if stored in an atmosphere saturated with benzene. None of the BDB*n* forms or their solutions in THF, EtOH, or MeOH are photochromic when irradiated with UV light from a medium-pressure mercury UV lamp, and no thermochromism was detected in solution.

2.2. Physicochemical Characterization and Theoretical Calculations. The thermal properties and the thermochromic transition behavior were investigated with differential scanning calorimeter (Pyris-1, Perkin-Elmer) equipped with an intercooler. The temperatures and heat flow were calibrated relative to the melting temperature (429.7 K) and heat of fusion (28.45 $J \cdot g^{-1}$) of pure indium. The heating and cooling rates were 2 or 10 $K \cdot min^{-1}$, respectively. The temperatures of solid−solid transition (T_{cc}) and melting (T_m) were taken as the peak points of the endothermic peaks. The heats of solid−solid transition (ΔH_{cc}) and melting (ΔH_m) were obtained from the endothermic peak areas. The entropies (ΔS_{cc} and ΔS_m) were calculated from the relations $\Delta S_{cc} = \Delta H_{cc}/T_{cc}$ and $\Delta S_m = \Delta H_m/T_m$.

The temperature-variable UV−visible spectra in the solid state were recorded on a ColorEye 3100 UV/vis reflectance spectrophotometer (Gretag Macbeth, USA), equipped with a custom-designed temperature controlling accessory. The pristine BDB*n* crystals were sandwiched between two glass plates and used to record the spectra in reflection mode. A thermocouple was introduced into the heating element and close to the sample in order to monitor the temperature, and the temperature of the heating element was controlled externally. The heating and cooling were performed at discrete temperatures, in 10 K steps, each step taking about 5 min for equilibration. The absorption UV−visible spectra in solution were recorded at room temperature with a Hewlett-Packard 8453 diode-array spectrophotometer. Diluted solutions of each compound in approximately identical concentrations were prepared in acetonitrile and used for measurement. To test the effect of concentration, a series of six solutions were prepared for each compound by serial dilution. The two lowest-energy bands in the spectra of all compounds were identical and did not exhibit observable dependence on the concentration over the detectable concentration range, which confirmed that the respective transitions are intramolecular and originate from the identical chromophore. The spectra shown in Figure 4 correspond to similar concentrations, because of the identical path length and similar molar absorption coefficients expected from the identical chromophore in each case.

The infrared spectra of polycrystalline BDB*n* in KBr pellets were recorded on a FTIR 2000 spectrometer (Perkin-Elmer). Each infrared spectrum was obtained by averaging 32 scans with a resolution of 4 cm^{-1}.

The excited states of BDB2 were calculated on the optimized structure by considering only configurations with single excitations (CIS).[8] The calculations were performed with the Gaussian03 program suite.[9] The molecular geometry of BDB2 was optimized without restraints within the density functional theory, at the B3LYP/6-31G(d) level, and the stationary points were checked for minima by subsequent harmonic vibrational analyses.

2.3. Structure Determination and in Situ HT X-ray Diffraction. The RT single crystal X-ray diffraction data for phase identification were collected in ω-scan mode with APEX2 diffractometer (Bruker AXS),[10] using Mo Kα X-rays obtained from a rotating anode source, a confocal multilayer X-ray mirror as monochromator, and CCD as area detector. The integrated and scaled data[10] were empirically corrected for absorption effects with SADABS.[11] The structures were solved by using direct methods[12] and refined on F_o^2 with SHELXL.[13] All non-hydrogen atoms were treated anisotropically, and all aromatic hydrogen atoms were included as riding bodies. Depending on the data quality, either the amino and hydroxyl hydrogen atoms were included as riding bodies or otherwise they were located and refined based on their positions in the difference maps. Because of the spontaneous desolvation in air, the diffraction data of the benzene solvate of BDB5 were collected from a very thin yellow plate sealed in low-absorbing capillary with plugs of crystallization solution on both sides of the crystal.

TABLE 1: Designation of the RT and HT Polymorphs and Solvates of BDB*n* ($n = 2-5$) Described in This Work

	notation of the form	
compound	room temperature	high temperature
BDB2	A[a]	C
	B[a]	
	D[a]	
BDB3	A[a]	B
BDB4	A[a]	C
	B[a]	
BDB5	A[a]	
	B[a,b]	

[a] Characterized by single crystal X-ray diffraction. [b] Benzene solvate.

In the in situ HT X-ray diffraction experiment, the data were collected at 293 and 370 K (the temperature values are corrected for the difference between the measured and the actual temperature at the crystal position determined independently by using calibration standards and direct measurement) from a prismatic crystal of BDB3 obtained by recrystallization from EtOH. Mo Kα X-rays were used with an APEX2 diffractometer (Bruker AXS), equipped with CCD detector and a specially designed double-gas heating device with externally controllable temperature of the nitrogen gas.[14] After the RT data were collected at 293 K, the temperature of the crystal was increased slowly to 370 K, below the solid−solid phase transition, where the diffracting ability of the crystal was completely preserved, and a second data set was collected at that temperature using identical strategy. The RT and HT data were treated as described above. The positions of all non-hydrogen atoms were assigned anisotropic parameters, and all H-atom positions, except for the two aromatic hydrogen atoms which were treated within the riding model, were located in the Fourier maps and refined without constraints.

3. Results and Discussion

3.1. Polymorphism and Structure Elucidation of the RT Phases. Extensive polymorph screening of the four BDB*n* compounds afforded seven RT polymorphs and one solvate as a large number of crystal habits (Table 1; microscopic images of the crystals with different habits are deposited as Supporting Information, Figure S1). In addition to forms A and B of BDB2, the crystal structures of six new forms of BDB2−BDB5 were determined in this work. Plots of the molecular structures are presented in Figure 2 and the respective crystallographic data are listed in Table 2 together with the two previously reported forms of BDB2. The IR spectra of the new forms (deposited as Supporting Information, Figure S2) confirm the presence of strongly hydrogen bonded OH groups, in addition to NO_2 groups and hydrogen bonded NH groups. Depending on the form, the color of the BDB*n* crystals varies from faint yellow to deep yellow. The structures of two polymorphs of BDB2, orthorhombic *Pbca* (form A) and monoclinic $P2_1/n$ (form B), each having a single crystallographic molecule in the unit cell, were reported previously[15] and were also isolated and identified as the major modifications of BDB2 from several solvents in this study. From THF, however, concomitantly with form A, a minor fraction of a third polymorph of BDB2 (form D) was isolated. The crystals of form D are of monoclinic, $P2_1/n$ symmetry, but contrary to form B they contain *four* nonequivalent stacked molecules in the asymmetric unit, with one of the hydroxyl groups disordered over two positions. The powder diffraction pattern of form D simulated from the structure determined by single crystal diffraction (deposited as Supporting Information, Figure S3) confirmed that the structure is different from either of forms A and B, as well from the HT form C (vide infra). On the other hand, although BDB3 crystallizes as many different habits, the diffraction analysis confirmed that they are all structurally identical and correspond to a monoclinic $P2_1/c$ structure with a single independent BDB3 molecule in the unit cell. For BDB4, two polymorphs were isolated, triclinic $P\bar{1}$ (form A) and monoclinic $P2_1/n$ (form B), containing one and two independent molecules in the asymmetric unit, respectively. From most solvents, BDB5 was obtained as triclinic $P\bar{1}$ crystals (form A). From benzene, however, crystals of a very unstable orthorhombic $Pca2_1$ solvate of BDB5 were obtained (form B) which lose benzene and in the absence of solvent decay in less than an hour at RT. The 1:1 stoichiometry of the solvate was unequivocally established by the X-ray structure analysis.

3.2. Thermochromism and Thermally Induced Modifications of the Morphology of BDB*n* Crystals. Figure 3 shows the temperature effects on the UV−vis spectra of a heated crystalline sample of BDB2. The *gradual* color change from yellow to orange-yellow occurs within a well-defined temperature interval above RT, denoted regime I hereafter. The effect, pronounced well in the crystals of BDB2 and BDB3 (Figure 3, spectra A and C), is related to continuous shift of the red absorption edge caused by overall intensification of the complex of absorption bands with $\lambda_{max} \approx 480$ nm, without alteration of the relative intensity of the component bands. According to the calculated excitation energies of BDB2,[16] the strongest band which dominates the low-energy spectral region corresponds to *intra*molecular CT, mainly from the HOMO to the LUMO. Accordingly, this band is the lowest energy band in the spectra in acetonitrile solution (422 nm) and the only absorption in the visible region (the second lowest-energy band appears in the UV region, at 340 nm; Figure 4). The insensitivity of the band to the alkyl length and the concentration supports its assignment to intramolecular CT. As shown in Figure 4 with the optimized structure of BDB2 in the configuration with intramolecular hydrogen bond between the terminal hydroxyl groups, which corresponds to the molecular structure observed in the polymorph A, the HOMO is predominantly located on one of the amino groups and the two nitro-ipso carbon atoms, whereas the LUMO is centered around the opposite nitro group. Unlike what would be intuitively expected for an X-type CT system with short-alkyl substitution (e.g., the CT from amino half to the nitro half of the molecule in the case of DADNB), the asymmetry brought about by the conformational freedom of the alkyl substituents reorients the charge flow and the absorption excites diagonal CT across the molecule.

Except for BDB5 and form B of BDB4, which melt directly, further heating of the orange-yellow crystals of BDB2, BDB3, or BDB4 up to their melting points, denoted temperature regime II, results in sharp change of color to intense orange-red or brick red (Figure 3, spectra A, C, and E). Contrary to regime I, the color change in regime II is related to significant alteration of the relative band intensities and intensification of the band around 500 nm. The existence of two regimes of spectral change suggests qualitatively different mechanisms of the thermal effects on the structures of BDB2−4 and can be also readily inspected from the morphology of single crystals (Figure 1). Whereas heating in regime I affects neither the shape nor the three-dimensional structural order (as inspected from the diffraction patterns), heating in regime II results in significant changes in the morphology and apparent crystal disintegration

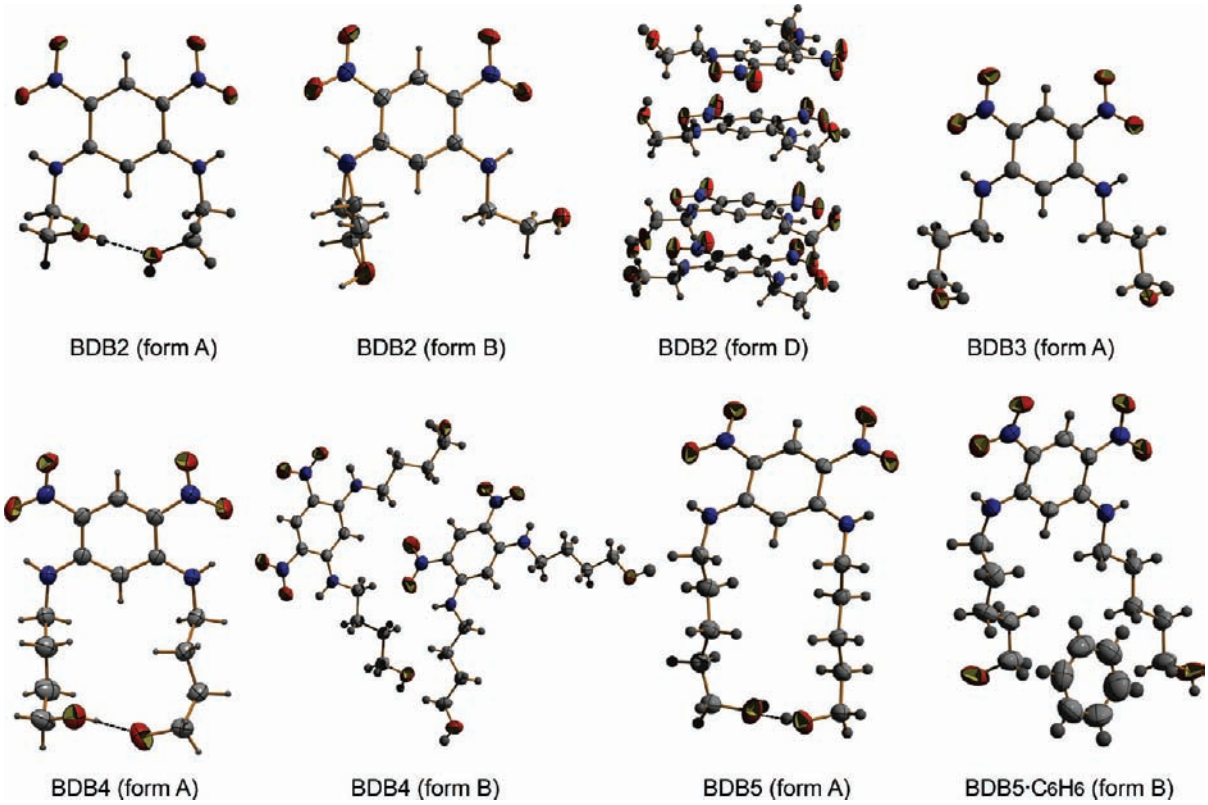

Figure 2. ORTEP-style plots of the molecular structures of crystalline BDB*n* compounds at RT (all non-H atoms are represented at 50% probability level. The structures of forms A and B of BDB2 are identical with the structures of these polymorphs determined previously.[3] Note that the molecules of forms A of BDB2, BDB4, and BDB5 are "locked" by one strong intramolecular hydrogen bond between the terminal hydroxyl groups, whereas the other molecules are "unlocked".

which is monitored as abrupt transformation of the discrete Bragg reflections into powder diffraction rings. By heating in regime II, the originally smooth, transparent, bright yellow faces of single crystals of BDB2 (form A) turn dark and opaque. The thermal treatment is also accompanied with readily observable bending at the longest axis, although the overall crystal integrity is retained. The deformation is plastic and the original crystal shape is not recovered even after cooling to RT. Although the crystallinity of the samples (BDB2, BDB3, and BDB4) is lost after the first complete cycle (Figure 1), the color of the yellow microcrystalline residue can be switched many times. The prismatic crystals of BDB3 (form A) also undergo permanent bending and darkening, but they usually crack and disintegrate into several parts. On the other hand, crystals of BDB4 (form A) undergo morphology changes mainly through "edge-softening" due to surface melting. The different morphology changes of heated BDB2, BDB3, and BDB4 single crystals in regime II clearly indicates differences in the thermal effects on the respective crystal structures.

3.3. Phase Transitions and Thermodynamic Properties. The DSC curves shown in Figure 5A and the respective transition temperatures, enthalpies, and entropies listed in Table 3 provide evidence that except for the two forms (A and B) of BDB5 and form D of BDB4 (the solvate decomposes, while the other two melt directly), in regime II all other forms undergo sharp endothermic solid−solid phase transitions to the respective HT phases. In addition, BDB3 undergoes two subsequent endothermic phase transitions, at 389 and 392 K. As shown in Figure 5B, the double peak of BDB2 in Figure 5A is due to the coexistence of the forms A and B at RT.

To investigate the thermal behavior of the HT forms of BDB*n* ($n = 2-4$; form C for BDB2 and BDB4, and form B for BDB3) corresponding to the respective mono-aci-nitro forms,[3] the reversibility of the solid−solid phase transitions was studied with several series of cyclic DSC experiments. The HT forms were first obtained in situ, by heating of the RT forms (first heating run) and holding the samples for 5 min at temperatures between T_{cc} and T_m (423, 403, and 394 K for BDB2, BDB3, and BDB4, respectively). The HT form was then cooled to 313 K and subsequently heated (second heating run) to the same temperature (Figure 6). It was confirmed[3] that by heating both RT forms of BDB2 (A and B) are converted to the same form (form C), albeit at different temperatures (127 and 140 K in the case of form A and form B, respectively). Comparison of the HT powder diffraction pattern of form C[3] with the simulated pattern of form D (Figure S3 in Supporting Information) ascertains that form D is different from the HT form C. The HT phases (forms C) of BDB2 and BDB4 do not exhibit any peaks during the first cooling run and the second heating run, and therefore the phase recovery from the HT phase to the RT phase does not occur immediately. Due to the very slow kinetics of the reverse phase transition, the HT phases C in crystals of BDB2 and BDB4 are trapped at RT away from equilibrium. Panels B and I of Figure 3 show that the recovery of the UV−vis spectrum of BDB2 proceeds very slowly and is not completed even after one day. On the contrary, the recovery of the RT phase (form A) from the HT phase (form B) of BDB3 is very rapid (Figure 3D), and the compound exhibits both phase transitions (exothermic peaks at 392 and 363 K) during the cooling and the second heating (endothermic peaks at 389 and 392 K). The hysteretic process related to the pair of lower temperature peaks at 363 and 389 K was identified as reoccurrence in regime II of the sharp thermochromic transition of the RT phase to the HT aci-nitro form which has been rapidly

TABLE 2: Crystallographic Data for BDB*n* (*n* = 2−5)

parameter	BDB2 (form A)[a]	BDB2 (form B)[a]	BDB2 (form D)	BDB3 (form A)	BDB4 (form A)	BDB4 (form B)	BDB5 (form A)	BDB5 (form B)
solvent	ethanol	acetonitrile	tetrahydrofuran	chloroform	ethanol	ethyl acetate	ethanol	benzene
empirical formula	$C_{10}H_{14}N_4O_6$	$C_{10}H_{14}N_4O_6$	$C_{10}H_{14}N_4O_6$	$C_{12}H_{18}N_4O_6$	$C_{14}H_{22}N_4O_6$	$C_{14}H_{22}N_4O_6$	$C_{16}H_{26}N_4O_6$	$C_{16}H_{26}N_4O_6 \cdot C_6H_6$
formula weight	286.25	286.25	286.25	314.30	342.36	342.36	370.41	448.52
temperature/K	293	293	293	293	293	293	293	293
wavelength/Å	0.71073	0.71073	0.71073	0.71073	0.71073	0.71073	0.71073	0.71073
crystal system	orthorhombic	monoclinic	monoclinic	monoclinic	triclinic	monoclinic	triclinic	othorhombic
space group	*Pbca*	$P2_1/n$	$P2_1/n$	$P2_1/c$	$P\bar{1}$	$P2_1/n$	$P\bar{1}$	$Pca2_1$
a/Å	17.4174(2)	10.453(5)	13.9814(3)	7.2445(12)	4.8071(3)	8.3906(19)	4.7244(2)	7.6093(8)
b/Å	7.01760(10)	9.464(5)	15.9511(3)	20.901(4)	10.6331(6)	14.517(3)	12.1071(4)	18.2086(18)
c/Å	19.3440(2)	12.557(5)	22.2275(4)	9.7813(16)	16.1500(9)	26.835(6)	15.6874(5)	17.2841(17)
α/deg	90	90	90	90	80.715(4)	90	84.553(2)	90
β/deg	90	102.551(5)	93.0190(10)	97.413(2)	83.144(4)	91.427(3)	87.211(2)	90
γ/deg	90	90	90	90	87.224(4)	90	88.585(2)	90
volume/Å^3	2364.39(5)	1212.5(10)	4950.27(17)	1468.7(4)	808.50(8)	3267.7(13)	892.01(6)	2394.8(4)
Z	8	4	16	4	2	8	2	4
ρ_{calc}/Mg·m^{-3}	1.608	1.568	1.536	1.421	1.406	1.392	1.379	1.244
μ/mm^{-1}	0.134	0.131	0.128	0.115	0.111	0.110	0.106	0.091
F(000)	1200	600	2400	664	364	1456	396	960
crystal size/μm	135 × 45 × 20	135 × 100 × 45	265 × 155 × 20	190 × 90 × 80	245 × 45 × 10	135 × 55 × 15	310 × 180 × 35	280 × 80 × 40
Θ range/deg	2.10−27.49	2.30−25.99	1.57−25.00	1.95−25.00	1.94−25.00	1.52−25.00	1.69−25.00	1.12−21.86
index ranges	$-22 \leftarrow h \leftarrow 22$	$-12 \leftarrow h \leftarrow 12$	$-16 \leftarrow h \leftarrow 16$	$-8 \leftarrow h \leftarrow 8$	$-5 \leftarrow h \leftarrow 5$	$-9 \leftarrow h \leftarrow 9$	$-5 \leftarrow h \leftarrow 5$	$-7 \leftarrow h \leftarrow 7$
	$-9 \leftarrow k \leftarrow 9$	$-11 \leftarrow k \leftarrow 11$	$-18 \leftarrow k \leftarrow 18$	$-24 \leftarrow k \leftarrow 24$	$-12 \leftarrow k \leftarrow 12$	$-17 \leftarrow k \leftarrow 17$	$-14 \leftarrow k \leftarrow 14$	$-19 \leftarrow k \leftarrow 19$
	$-25 \leftarrow l \leftarrow 25$	$-15 \leftarrow l \leftarrow 15$	$-26 \leftarrow l \leftarrow 26$	$-11 \leftarrow l \leftarrow 11$	$-19 \leftarrow l \leftarrow 19$	$-31 \leftarrow l \leftarrow 31$	$-18 \leftarrow l \leftarrow 18$	$-18 \leftarrow l \leftarrow 18$
reflns collected	41409	10595	112084	14020	16763	30523	13970	16230
independent reflns	2710 [R_{int} = 0.0360]	2379 [R_{int} = 0.0223]	8732 [R_{int} = 0.0666]	2596 [R_{int} = 0.0328]	2857 [R_{int} = 0.0446]	5730 [R_{int} = 0.0944]	3157 [R_{int} = 0.0372]	2863 [R_{int} = 0.0459]
refinement method	FMLS on F^2	FMLS on F^2	FMLS on F^2	FMLS on F^2	FMLS on F^2	FMLS on F^2	FMLS on F^2	FMLS on F^2
data/rests/params	2710/0/197	2379/4/220	8732/2/790	2596/0/215	2857/0/225	5730/0/457	3157/0/251	2863/1/305
goodness-of-fit on F^2	1.044	1.029	1.021	1.051	1.039	0.903	1.050	1.093
R indices [$I > 2\sigma(I)$]	$R_1 = 0.0367$	$R_1 = 0.0463$	$R_1 = 0.0443$	$R_1 = 0.0372$	$R_1 = 0.0490$	$R_1 = 0.0547$	$R_1 = 0.0394$	$R_1 = 0.0330$
	$wR_2 = 0.0901$	$wR_2 = 0.1299$	$wR_2 = 0.1027$	$wR_2 = 0.0929$	$wR_2 = 0.1172$	$wR_2 = 0.1320$	$wR_2 = 0.1003$	$wR_2 = 0.0751$
R indices (all data)	$R_1 = 0.0497$	$R_1 = 0.0528$	$R_1 = 0.0727$	$R_1 = 0.0485$	$R_1 = 0.0832$	$R_1 = 0.1683$	$R_1 = 0.0578$	$R_1 = 0.0564$
	$wR_2 = 0.0981$	$wR_2 = 0.1355$	$wR_2 = 0.1149$	$wR_2 = 0.0990$	$wR_2 = 0.1318$	$wR_2 = 0.1751$	$wR_2 = 0.1078$	$wR_2 = 0.0979$
diff. peak/hole/e·Å^{-3}	0.231/−0.203	0.224/−0.386	0.249/−0.215	0.140/−0.180	0.406/−0.191	0.296/−0.239	0.161/−0.168	0.188/−0.191
d(Ct···Ct)[b]/Å	3.795, 4.170	4.532	3.668, 3.629, 3.910, 4.385	3.581	4.807	4.137, 4.256	4.724	3.814

[a] The structures of these two polymorphs, redetermined in this study, are identical with our previous result (Lee, S. C.; Jeong, Y. G.; Jo, W. H.; Kim, H.-J.; Jang, J.; Park, K.-M.; Chung, I. H. *J. Mol. Struct.* **2006**, *825*, 70). [b] Distances between the benzene ring centroids shorter than 5 Å.

recovered during the first cooling. The pair of exothermic (cooling) and endothermic (heating) peaks at 392 K corresponds to a second phase transition without hysteresis which can be tentatively assigned to conformational changes of the alkyl groups of the aci-nitro form. The very narrow temperature interval of existence of this metastable form, however, precluded its identification.

3.4. Structural Basis of the Gradual BDB-Type Thermochromic Change. To unravel the mechanism of the gradual thermochromic change of BDB crystals above RT, a single crystal of BDB3 in form A was subjected to in situ HT single crystal X-ray diffraction by very slow heating to 370 K, below the first phase transition point T_{cc}. The relevant details of the structure at 293 and 370 K (the temperature values are corrected), are plotted in Figure 7. The heated crystal exhibited a clear color change from pale yellow to orange. Heating to 370 K results in 1.81% increase of the unit cell volume (from 1473.20(3) to 1499.844(91) Å^3), mostly owing to cell expansion along the $\pi-\pi$ stacking direction, which is quasi-parallel to the *a*-axis that stretches +1.38% (from 7.2459(11) to 7.3457(3) Å). The other two axes are relatively less affected; *b* stretches +0.55% (from 20.9361(2) to 21.0510(7) Å and *c* shrinks −0.11%, from 9.7928(1) to 9.7826(4) Å). Such values are not unexpected if the thermal effects on the lattices of other one-dimensional systems are considered.[5h] However, it is important to note that the relative changes between the *a*, *b*, and *c* axes in the crystal of BDB3 are quite different: the crystal stretches much more along *a* than it stretches along *b* and it shrinks along *c*. The monoclinic $P2_1/c$ symmetry of the crystal is preserved at 370 K and except for the increased thermal motions of the atoms, the molecular structure at 370 K remains nearly identical to that at 293 K. As expected from the very small rotational barrier, the thermal motions of the nitro groups are significantly increased at RT, although the O(nitro)···N(amino) distances remain almost constant, if the standard deviations are considered (O1···N3 = 2.6501(13) Å at 293 K and 2.6505(18) Å at 370 K; O4···N4 = 2.6415(14) Å at 293 K and 2.6373(19) Å at 370 K). No evidence of electron density surplus that would support eventual partial proton transfer from the amino to the nitro group was observed in the F_o-F_c maps, confirming that the nitro tautomer of the molecule is completely preserved up to 370 K. Instead, the anisotropic cell expansion is reflected in *expansion* of 1.1% (from 3.889 to 3.932 Å, calculated on the respective benzene centroids) and 0.8% (from 3.581 to 3.609 Å) of the two inter-ring distances within the stacks (Figure 7, structures c and d). If the structure at HT is considered, the macroscopic bending observed with heated crystals of BDB3 can be expected by the strong (more than twice) expansion of the cell along one of the two smaller axes of the crystal (100) relative to expansion along the longest axis corresponding to the (010) direction. The HT structure ascertains that the color change from yellow to orange-yellow in regime I is caused solely by changes in the intermolecular interactions. Due to the strong $\pi-\pi$ interactions, at RT the intramolecular CT is delocalized and effectively channeled through the intermolecular contacts. At higher temperature, the increased distance between the stacked rings effectively deactivates the intermolecular pathways for deexcitation. As a consequence, the CT becomes localized within the individual molecules and the oscillator strength of the low-energy intramolecular CT bands increases,

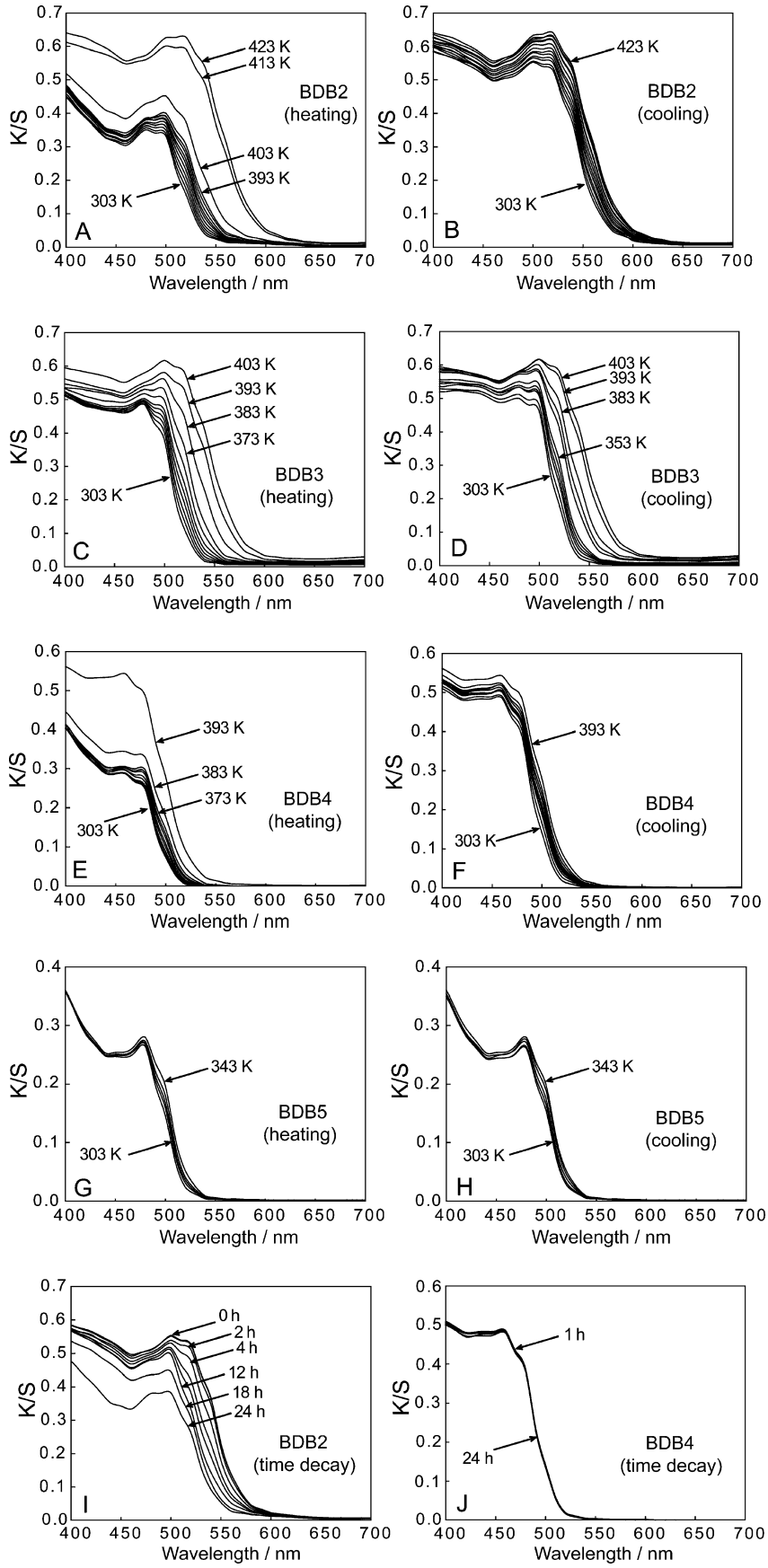

Figure 3. Thermal effects on the UV−visible reflectivity spectra of BDB2−BDB5 in the solid state (panels A−H) and temporal profile of the spectra of BDB2 and BDB4 after one heating−cooling cycle (panels I and J). The overall increase of the absorption of cooled BDB2 and BDB4 probably appears as a result of the very slow dynamics of the recovery of the room temperature phase, formation of multiple phases or partial melting (due to the close temperature of the solid−solid and solid−liquid transitions).

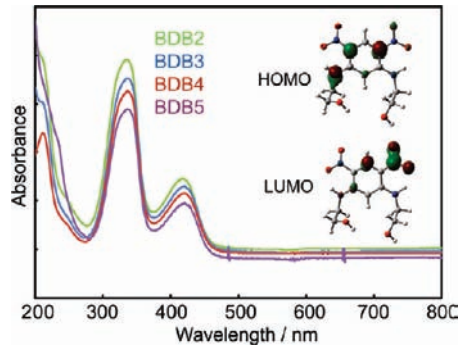

Figure 4. UV−visible absorption spectra of diluted solutions of BDB2−BDB5 in acetonitrile. Inset: plots of the frontier orbitals of BDB2 in the "locked" conformational minimum (extracted from the electron wave function of the B3LYP/6-31G(d)-optimized structure).

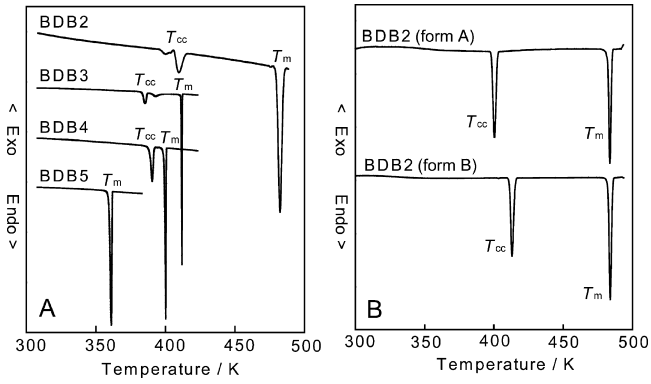

Figure 5. (A) DSC curves of the first heating run above RT ($\beta = 2$ K·min^{-1}) of form A BDBn crystals ($n = 2-5$). The double T_{cc} peak in the case of BDB2 is a result of coexistence of both RT forms (A and B). (B) DSC curves of the first heating run of the pure forms A and B of BDB2.

TABLE 3: Phase Transitions and Thermodynamic Properties of the RT Forms of BDBn ($n = 2-5$)

	T_{cc}/K	ΔH_{cc}[a]	ΔS_{cc}[b]	T_m/K	ΔH_m[a]	ΔS_m[b]
BDB2 (form A)[c]	400	23	58	483	24	50
BDB2 (form B)[c]	413	19	46	483	24	50
BDB2 (form D)	410	11	27	483	24	50
BDB3 (form A)	386	6	16	412	23	56
BDB4 (form A)	391	14	36	400	30	75
BDB4 (form B)				400	30	75
BDB5 (form A)[d]				361	45	125

[a] In kJ·mol^{-1}. The values are rounded to ±0.5. [b] In J·mol^{-1}·K^{-1}. The values are rounded to ±0.5. [c] The data of forms A and B of BDB2 were taken from ref 3. [d] The benzene solvate of BDB5 (form B) is very unstable at RT and therefore its thermal properties were not studied.

which appears as intensification of the absorption bands and red shift of the visible absorption edge (Figure 3, panels A and C).

From the above inference that the gradual thermochromism in regime I is caused by changes in the stacking distance, it can be concluded that the polymorphs of BDBn compounds in which the molecules are separated beyond the usual stacking distances should not exhibit gradual color change by heating. Inspection of the $\pi-\pi$ stacking distances in Table 2 unravels that such cases are form B of BDB2, forms A and B of BDB4, and form A of BDB5. As shown in Figure 1, while crystals of forms A of BDB2 and BDB3 are clearly thermochromic, forms

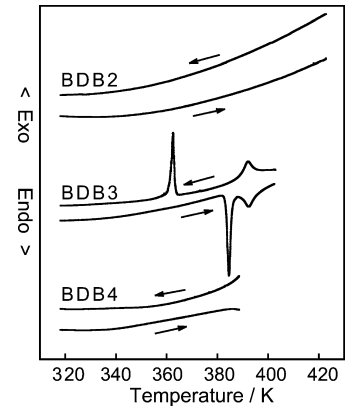

Figure 6. DSC curves of the first cooling run and the second heating run of in situ produced HT phases of BDBn ($n = 2-4$, $\beta = 2$ K·min^{-1}).

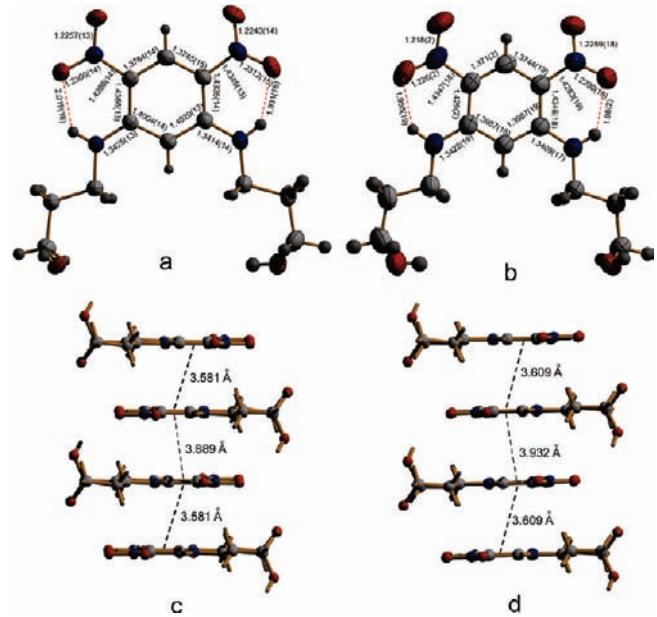

Figure 7. Comparison of the molecular (a, b) and packing (c, d) structures of BDB3 (from EtOH) at 293 K (a, c) and 370 K (b, d). The values in (a, b) and (c, d) represent the distances (in angströms) between the atoms and the benzene ring centroids, respectively.

A of BDB4 and BDB5 do not exhibit apparent gradual thermochromism (form B of BDB2, not shown in Figure 1, does not exhibit gradual thermochromism either). Inspection of the UV−vis spectra in Figure 3 supports such an observation: if compared to BDB2 and BDB3, where the absorption edge red shifts to >550 nm, the shift of edge of BDB4 and BDB5 by heating and cooling in regime I is much smaller and <550 nm. Therefore, the differences in the gradual thermochromic activity of the various BDBn forms indirectly confirm the mechanism suggested based on HT X-ray diffraction.

3.5. Structural Mechanism of the Sharp BDB-Type Thermochromic Change. The reverse proton transfer from the thermally created aci-nitro group to the imino nitrogen atom and the recovery of the RT forms of BDB2 (A and B) from the HT phase C were studied with a series of DSC experiments. Pure form C, obtained by annealing of the RT form for 5 min at 423 K, was quickly transferred and stored for a period of time in an isothermal environment, at temperature T_i (258, 280, 303, 323, or 343 K), whereupon slow transition of the HT form C to the RT form(s) took place. The identity of the recovered RT phase was confirmed by a second heating run. During the

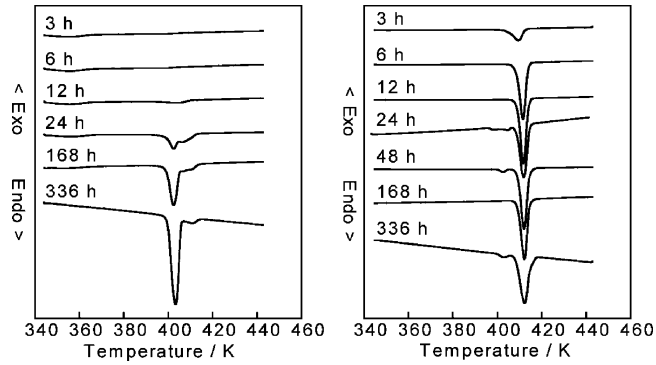

Figure 8. DSC curves recorded during the *second* heating ($\beta = 2$ K·min^{-1}) of precooled HT phase C of BDB2. The sample was first held for 5 min at 423 K to obtain form C, cooled to 280 K (plot on the left) or at 303 K (plot on the right), and maintained for the designated period of time before the second heating run.

second heating, the samples which were stored at $T_i = 258$ or 280 K exhibit a strong endothermic DSC peak at 403 K that corresponds to transition of form A to form C ($T_{cc} = 400$ K) and a small peak at 413 K from the transition of form B to form C ($T_{cc} = 413$ K). A typical series of profiles shown in Figure 8(left) shows very slow recovery of both RT phases, mostly of form A, from the cooled form C. Remarkably, the peak at 403 K intensifies with the time during which the sample had been stored at low temperature. If, however, the cooled form C is stored at $T_i = 303$, 323, or 343 K, the main endothermic peak during the second heating appears at 413 K—the temperature corresponding to transition of form B to form C. Again, the peak at 413 K increases with the storage time, as demonstrated with the DSC curves shown in Figure 8(right).

These experiments show that the recovery of RT phases A and B created in situ from the HT phase C of BDB2 is a very slow process which involves competition between two parallel transitions: C-to-A and C-to-B (both forms A and B are stable within the temperature range used for storage so that significant conversion between them is not expected at the time scale of the experiments). At lower temperatures ($T_i = 258$ and 280 K) the major product of the transition of form C is form A, while higher temperatures ($T_i = 303$, 323, or 343 K) favor the formation of form B. The ΔH_t values from the DSC curves obtained during the second heating run were employed to calculate the normalized enthalpies $X_t = \Delta H_t/\Delta H_{cc}$, where $\Delta H_{cc} = 81$ J·g^{-1} for form A (that is, for $T_i = 258$ or 280 K) and $\Delta H_{cc} = 66$ J·g^{-1} for form B (for $T_i = 303$, 323, or 343 K). The time profiles of X_t in Figure 9 (the respective values are deposited as Table S1 in the Supporting Information) show very long lifetime of the HT (aci-nitro) form C; the transition to the RT (nitro) form A has not completed even after 320 h. Contrary to what would be normally expected for a thermally activated process, the rate constants, calculated from the recorded portion of the plot as 1.3×10^{-6} s and 2.1×10^{-6} s^{-1} at 280 and 258 K, respectively, decrease with increasing the temperature (all rate constants were calculated assuming first-order kinetics and formation of only one product). This effect is a result of the increasing stability of B relative to A at higher temperatures. The form B is obtained from C more rapidly above 280 K, with estimated rate constants on the order of 10^{-7} s^{-1} and decreasing with the increase of the temperature. At 303 K the process of transition of C to B is completed within 20 h from the cooling. The decreasing trend of the phase transition rate continues even in the region where form B is created, which is now due to shift of the equilibrium to the HT form C that is more stable at

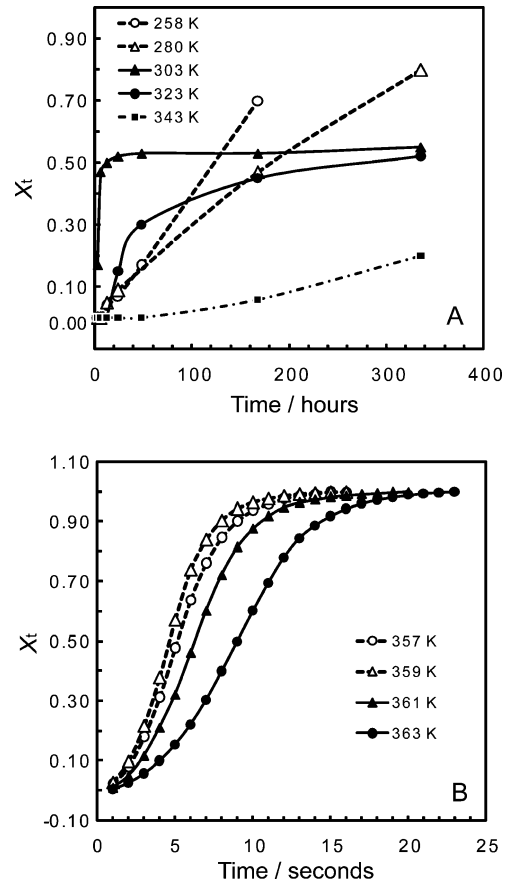

Figure 9. (A) Kinetic plots of transformation of the HT form C of BDB2 to the RT forms A and B. X_t is defined as $\Delta H_t/\Delta H_{cc}$, where $\Delta H_{cc} = 81$ J·g^{-1} for form A ($T_i = 258$ or 280 K) and $\Delta H_{cc} = 66$ J·g^{-1} for form B ($T_i = 303$, 323, or 343 K). (B) Kinetic plots of transformation of the HT form B of BDB3 to the RT form A (the different curves are related to different values of the transformation temperature T_i shown in the legend). The X_t values were calculated according to eq 1.

higher temperatures. Because the point for stability resolution of phases A and B is between 280 and 303 K, these two modifications are of similar stability at RT, in accordance with the observation that depending on the solvent, both form A and form B were obtained as pure or concomitant phases by crystallization at RT.

The rapid transformation of BDB3 from its HT form B to the RT form A (relative to BDB2) necessitated a different DSC strategy for quantification of its kinetics. Form B of BDB3 that has been produced in situ from form A by heating and storing for 5 min above the thermochromic transition temperature T_{cc} (390 K), was rapidly cooled to the temperature of isothermal transformation T_i and kept isothermally at T_i during 10 min while the enthalpy of transformation was recorded as a function of time. The time profiles of the phase transition enthalpies ΔH_t after time t determined with eq 1 are plotted in Figure 10, and the respective values are deposited as Table S2 in Supporting Information. In striking contrast with BDB2, the thermal recovery of the RT nitro form of BDB3 from its HT aci-nitro form is extremely fast and the process is completed in less than 15 s, with rate constants between 0.4 s^{-1} (357 K) and 0.3 s^{-1} (363 K). Similarly to the initial stage of conversion of the BDB2 forms (Figure 9(left)), the isotherms of phase transition of BDB3 at various temperatures (Figure 9(right)) have sigmoidal shape and the rate decreases with increasing temperature.

$$X_t = \frac{\int_0^t (dH/d\tau)\, d\tau}{\int_0^\infty (dH/d\tau)\, d\tau} \quad (1)$$

Similarly, BDB4 was converted to its HT form C by heating of the RT phases and holding for 5 min at 394 K, between T_{cc} and T_m. Subsequent cooling of form C to $T_i = 293$ K and a second heating did not exhibit any exothermic peaks, even when the sample was stored for 7 days at 293 K. This result means that contrary to BDB2 and BDB3, the recovery rate of the thermochromic phase of BDB4 is extremely slow.

3.6. Correlation of Thermal Effects with the Crystal Structures. According to the results from the HT XRD analysis of BDB3 discussed above, the gradual thermochromism of BDB*n* crystals corresponds to alteration of the intermolecular $\pi-\pi$ stacking distance, which is related to the anisotropic thermal expansion of the lattice. Unlike other thermochromic systems, such as are for instance the well investigated overcrowded enes[17] and thermochromic anils,[18] as well as some other recently reported systems,[19] where heating or cooling causes population/decay of the thermochromic product due to molecular distortion(s), enol−keto tautomerism or dimerization, although the BDB*n* compounds do undergo clear thermochromic change in regime I, they do not exhibit any significant alteration in the molecular geometry or shifts in the tautomeric equilibrium involving the amino proton. Instead, the molecules remain as their nitro tautomers, with intramolecularly hydrogen-bonded nitro groups and the proton transfer does not occur until sufficient thermal energy has been provided for a proton jump along one of the two intramolecular hydrogen bonds (subsequent, second proton transfer event is prevented by the fixation of the resonance structure; Scheme 2). This is somewhat expected if the energy profile for the nitro−aci-nitro equilibrium is considered, which is much steeper and it is also flatter on the side of the acidic form than the respective profile for the enol−keto exchange.[6]

Even if substituted with short alkyl chains, in the solid state conjugated molecules such as BDB*n* are usually nearly planar[20] and the side chains tend to adopt zigzag conformation and to remain coplanar with the aromatic ring. Since the hydrogen-bond-forming groups of BDB*n* in such a case would be situated close to the molecular plane, the three-dimensional supramolecular structures are normally dominated by stacking interactions. The thermal effects on the structure and crystal morphology during the first heating of BDB*n* crystals from their RT forms and through regimes I and II correlate well to the structures at RT. The pronounced tendency for disintegration of crystals of BDB3 relative to BDB2 and BDB4, for instance, is related to strong anisotropy in the thermal expansion, as confirmed by HT XRD analysis in this work. A second reason may be pronounced structural dissimilarity between the respective RT and HT phases. Relative to the shorter alkyl members BDB2 and BDB3, BDB4 and BDB5 exhibit liquid-crystal-like behavior, which is brought about by increasing length of the alkyl chains. The increasing effect of the flexible hydrophobic chains on the packing is reflected in the calculated crystal densities, which decrease very regularly in the order BDB2 (A) > BDB2 (B) > BDB3 (A) > BDB4 (A) > BDB4 (B) > BDB5 (A) > BDB5 (B) (Table 2). The partial disorder observed in the structures of forms B and D of BDB2 may be also related to the looser packing relative to form A. As a result of decreasingly dense packing, the structure of the highest member, BDB5, becomes sufficiently flexible to accommodate a benzene molecule (form B) which is held loosely in the lattice by two weak trans-oriented C−H···π interactions (d(C···π) = 3.860 and 3.922 Å; d(H···π) = 3.05 and 3.07 Å) and easily leaves the crystal even at RT. Correspondingly, whereas the HT forms of BDB2 and BDB3 melt sharply, in regime II the crystals of BDB4 "soften" just before the complete melting, while the highest member of the series BDB5 melts without any observable crystal deformation or phase transition (Figure 1). In general, the kinetic experiments show that the order of rates for recovery of the RT forms from the HT forms is BDB3 > BDB2 > BDB4. The reversed phase transition of BDB4 is probably an extremely slow process, and the HT form is practically stable at RT.

The temperatures of the HT solid−solid transitions (T_{cc}) and melting (T_m) decrease with increasing number of methylene groups in the alkyl chain (Figure 11). Relative to T_{cc}, the T_m values fall off more rapidly with the alkyl chain length and consequently the temperature gap between the two transitions ($T_{cc}-T_m$) decreases. This is expected from the notion that the solid−solid phase transition is triggered by an intramolecular event, proton jump between the proximate amino and nitro groups, and thus it is less affected by the structure of the remainder of the molecules and the crystal packing relative to the melting. The melting, on the other hand, depends critically on crystal packing, which is related to the molecular size and shape, and the intermolecular interactions. Accordingly, the T_m of the highest member of the series, BDB5, is lowered below T_{cc} and the compound melts without preceding solid−solid phase transition. The enthalpies and entropies (ΔH_{cc} and ΔS_{cc} in Table 3) related to the solid−solid transition of BDB3, with odd number of alkyl carbon atoms, are lower than those of the even-carbon members of the series, BDB2 and BDB4, which appears to resemble the odd−even effect commonly observed with the thermal behavior of liquid crystals.[21] On the contrary, the melting temperatures do not exhibit an odd−even effect: the enthalpies of BDB2−4 are nearly identical, the entropies increase with the alkyl length, and BDB5 has much larger values of both the enthalpy and entropy than the other members. There are, however, additional observations which albeit less quantitatively, seem to be in accordance with the odd−even effect: while two solvent-free polymorphic modifications exist as stable forms at RT for each of the even members BDB2 and BDB4, aside from the benzene solvate of BDB5, only one polymorph could be obtained of each of the odd members BDB3 and BDB5.

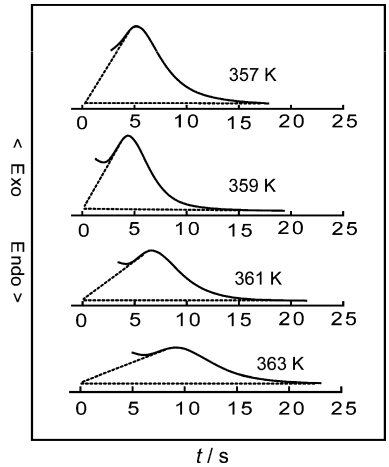

Figure 10. DSC isotherms of the transformation of HT form (B) of BDB3 produced in situ from form A and rapidly cooled to the designated temperature.

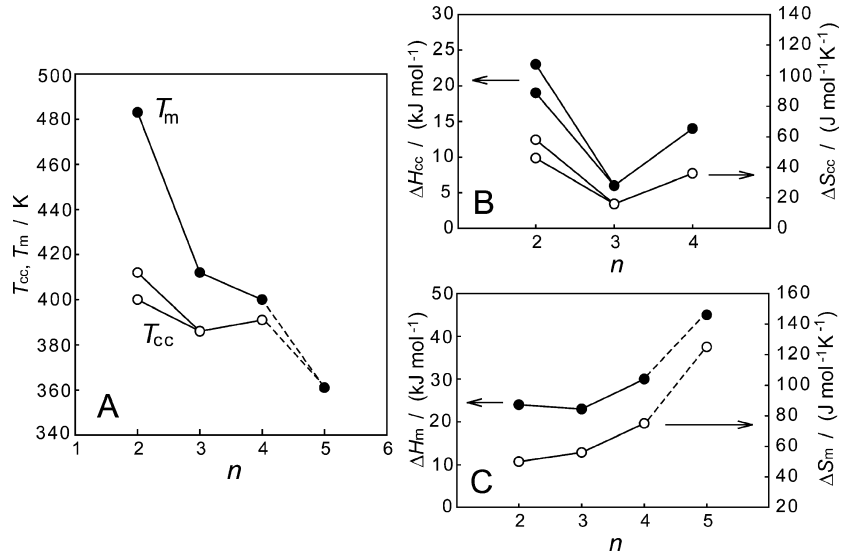

Figure 11. Temperatures (A) and thermodynamic parameters (B, C) of the phase transitions of BDB*n* ($n = 2-5$) during the first heating run, as function of the number of methylene groups (*n*).

As will be explained further in this article, this may be related to the number of favorable conformations of the alkyl chains, since the aromatic part of the molecule is common to all compounds.

The unfortunate disintegration of crystals of all studied samples in regime II precluded structure determination of the HT phases by HT single crystal X-ray diffraction. Therefore, we were not able to compare their HT structures directly with the thermoanalytical data. In absence of structural data on the HT phases, the RT phases were compared to investigate the reasons behind the different thermal behavior of BDB3 from BDB2 and BDB4. Polymorphism, in general, has been increasingly recognized for its great potential for elucidation of structural−property relationships, because it provides information both on structural preferences and properties of the same molecule in various well-defined molecular environments.[22] The preferred evolution of forms A or B of BDB2 which was observed from the slow transformation from form C at different temperatures (Figure 9) may be related to the hydrogen bonding of their alkyl arms (Figure 2). The alkyl arms of BDB2 in form A are closed and the molecule is locked in cyclic conformation by a single strong intramolecular hydrogen bond between the terminal hydroxyl groups (d(O···O) = 2.812 Å), and thus only one arm is available as donor (d(O···O) = 2.752 Å) for intermolecular hydrogen bonding, while the other one acts only as acceptor (d(O···O) = 2.752 Å). In form B, the substituent arms are pointing away from each other and therefore they are open, the molecule is "unlocked", and each of the two hydroxyl groups acts simultaneously as donor and acceptor for intermolecular hydrogen bonds with neighboring molecules (d(O···O) = 2.746 and 2.893 Å). All four independent molecules in form D BDB2 are unlocked. As the two alkyl chains naturally tend to adopt zigzag conformation (which becomes apparent with the higher members) and they are of equal length, whether molecular locking will occur or not during crystallization depends on the molecular conformation at the link between the amino group and the alkyl chains: if the alkyl groups flip out of the aromatic plane and align quasi-perpendicular to it, because of the equal length they are expected to meet at their ends to form a strong intramolecular hydrogen bond O−H···O with their hydroxyl groups, which ultimately locks the molecule. If, however, the conformation at the amino linkages retains at least one of the arms within the plane of the aromatic ring, the hydroxyl groups will point away from each other and the molecule will remain unlocked.

Rather than being a static observation, the dynamic nature of the locking−unlocking mechanism in BDB*n* crystals is actually related to the kinetics of the phase transition in the solid state, which is particularly well illustrated by considering the reversible phase transition of BDB2. As described above, depending on the temperature of isothermal aging, either form A or form B can be obtained from the HT form of BDB2. These two forms can be resolved around RT, with form A being the preferred product below and form B above RT. Because forms A and B correspond to the respective locked and unlocked conformations of the same molecule, this means that the molecular locking during the transition from the HT phase can be simply controlled by adjustment of the temperature. It should be noted that the forward and reverse RT-HT phase transitions are of solid−solid type, meaning that the whole process of phase recovery and the associated thermally controlled molecular locking proceed in the solid state. Once the molecule has been recovered at RT as the desired conformation, the phase transition of BDB2 can be repeated by a heating−cooling cycle, and the molecule can be trapped again in the same or in the other conformation. The stability difference between forms A and B thus corresponds to that between the locked and unlocked molecular conformations as thermodynamically and kinetically preferred product of the transition, respectively. This conclusion can be generalized as demonstration of the intramolecular hydrogen bonding as thermodynamically preferred (lower energy) relative to the intermolecular hydrogen bonding as kinetically preferred (higher entropy) process.

Due to the longer chain length and the odd number of carbon atoms in the structure of BDB3, the two arms are too far apart for formation of intramolecular hydrogen bond, so that the molecule remains unlocked and both groups act simultaneously as donor and acceptor to neighboring molecules (d(O···O) = 2.772 and 2.728 Å). In fact, in the crystal of BDB3 the two hydrogen bonded arms are bridged by other two hydroxyl groups from neighboring molecules in a head-to-tail arrangement, forming zigzag hydrogen bonded chains of molecules in a staircase-like fashion. Therefore, in lack of ability for intramolecular bonding, the hydrogen bonding potential in the crystal is

saturated by intermolecular hydrogen bond formers. The very different rates for recovery of the RT phases of BDB3 and BDB2 cannot be explained entirely until the crystal structures of the respective HT aci-nitro forms are resolved. Similarly with BDB2, the next even member, BDB4 also exhibits different molecular conformations in the two RT polymorphs: a conformation locked with a strong hydrogen bond (d(O···O) = 2.681 Å) between the two arms in polymorph A, and an unlocked conformation with spatially divergent arms in both crystallographically independent molecules of polymorph B (Figure 2). Locked conformation with zigzag arms is also observed in form A of BDB5, with hydrogen bonded terminal hydroxyl groups (d(O···O) = 2.694 Å). In form B BDB5, although one of the arms has a kink in the middle and is viable for closure, the other arm lies in the aromatic plane and points away, so that the molecule ultimately remains unlocked. The perturbation in this structure relative to form A and the inability for closure is imposed by the guest benzene molecule, which introduces significant freedom in the packing, as inferred from the very low density. Consequently, the BDB5 molecule in the crystal of form B represents an intermediate between two typical conformations, locked noncoplanar and unlocked coplanar.

4. Conclusions

The 1,3-bis(hydroxyalkylamino)-4,6-dinitrobenzenes BDBn (n = 2−5), bis(hydroxyalkyl) analogues of the intramolecular CT system DADNB, are a new class of organic thermochromic compounds which exhibit both polymorphism and reversible thermochromic change between yellow and orange or red forms in the solid state. The polymorphism is expressed by locking of the alkyl arms by hydrogen bonding at their hydroxyl termini, which decreases their potential for intermolecular interactions. In the locked molecular conformation, the alkyl arms orient quasi-perpendicular to the aromatic rings, whereas in the unlocked conformation they tend to align within the aromatic plane. The solid-state thermochromism of BDB-type is due to two subsequent processes: above RT, the oscillator strength of the low-energy intramolecular CT is enhanced by thermally continuous process of localization of the transitions caused by decreased aromatic stacking. At higher temperatures, discontinuous phase transitions occur, supposedly related to proton transfer along the intramolecular amino−nitro hydrogen bonds. If cooled to RT, the HT phases of different forms exhibit very different lifetimes, extending from an order of days in the case of BDB2 and BDB4 to several seconds in the case of BDB3. The aci-nitro form can be kinetically trapped as a metastable phase in the solid state at temperatures close to RT. Comparison with BDB3, which at RT can exist only in its unlocked conformation, unraveled that the extended lifetimes of the metastable HT phases of BDB2 and BDB4 can be related to their locked conformations. A particularly interesting case is the phase recovery of the RT phases from the HT phase of BDB2, where the molecule is recovered in its locked conformation (form A) or unlocked conformation (form B) depending on the temperature: the locked conformation appears more kinetically stable and is preferred at lower temperatures, while the unlocked conformation is more stable at higher temperatures. Because the whole process proceeds in the solid state and is completely reversible, the results present direct evidence of reversible thermally induced molecular locking. The kinetic resolution of the two forms can be interpreted and generalized in view of the intramolecularly hydrogen bonded conformation being a thermodynamically preferred product, versus the intermolecularly hydrogen bonded conformation as kinetically preferred product of the same molecule during the solid−solid phase transition.

Acknowledgment. This study was performed by support of the "Frontier Research Base for Global Young Researchers" program of the MEXT of the Japanese Government.

Supporting Information Available: Images of the crystals of BDBn (Figure S1), FTIR spectra (Figure S2), simulated powder diffraction patterns (Figure S3), kinetic data (Tables S1 and S2), Cartesian coordinates of the optimized structure of BDB2 (Table S3), X-ray crystallographic data for BDB3 at two different temperatures (Tables S4−S11), X-ray crystallographic files (CIF), and complete ref 9. This material is available free of charge via the Internet at http://pubs.acs.org.

References and Notes

(1) (a) Li, H.-P.; Han, K.; Tang, G.; Shen, X.-P.; Wang, H.-T.; Huang, Z.-M.; Zhang, Z.-H.; Bai, L.; Wang, Z.-Y. *Chem. Phys. Lett.* **2007**, *444*, 80. (b) Tomonari, M.; Ookubo, N. *J. Mol. Struct.: THEOCHEM* **1998**, *451*, 179. (c) Tomonari, M.; Ookubo, N.; Takada, T. *Chem. Phys. Lett.* **1997**, *266*, 488. (d) Nalwa, H. S.; Watanabe, T.; Miyata, S. *Adv. Mater.* **1995**, *7*, 754. (e) Nalwa, H. S.; Watanabe, T.; Miyata, S. *Opt. Mater.* **1993**, *2*, 73.

(2) Wortmann, R.; Lebus-Henn, S.; Reis, H.; Papadopoulos, M. G. *J. Mol. Struct.: THEOCHEM* **2003**, *633*, 217.

(3) Lee, S. C.; Jeong, Y. G.; Jo, W. H.; Kim, H.-J.; Jang, J.; Park, K.-M.; Chung, I. H. *J. Mol. Struct.* **2006**, *825*, 70.

(4) Lee, S. C.; Jeong, Y. G.; Jang, S. H.; Jo, W. H. *Fibers Polym.* **2007**, *8*, 234.

(5) (a) Naumov, P.; Sakurai, K. *Cryst. Growth Des.* **2005**, *5*, 1699. (b) Naumov, P.; Sakurai, K.; Ishikawa, T.; Takahashi, J.; Koshihara, S.; Ohashi, Y. *J. Phys. Chem. A* **2005**, *109*, 7264. (c) Naumov, P.; Jovanovski, G.; Sakurai, K. *Cryst. Growth Des.* **2006**, *6*, 815. (d) Naumov, P.; Sakurai, K.; Asaka, T.; Belik, A. A.; Adachi, S.; Takahashi, J.; Koshihara, S. *Eur. J. Inorg. Chem.* **2006**, 1345. (e) Naumov, P.; Sakurai, K.; Asaka, T.; Belik, A. A.; Adachi, S.; Takahashi, J.; Koshihara, S. *Chem. Commun.* **2006**, 1491. (f) Naumov, P.; Sakurai, K.; Asaka, T.; Belik, A. A.; Adachi, S.; Takahashi, J.; Koshihara, S. *Inorg. Chem.* **2006**, *45*, 5027. (g) Naumov, P.; Makreski, P.; Jovanovski, G. *Inorg. Chem.* **2007**, *46*, 10624. (h) Naumov, P.; Hill, J. P.; Sakurai, K.; Tanaka, M.; Ariga, K. *J. Phys. Chem. A* **2007**, *111*, 6449. (i) Naumov, P.; Sakurai, K.; Tanaka, M.; Hara, H. *J. Phys. Chem. B* **2007**, *111*, 10373. (j) Naumov, P.; Yu, P.; Sakurai, K. *J. Phys. Chem. A* **2008**, *112*, 5810.

(6) (a) Scherl, M.; Haarer, D.; Fischer, J.; DeCian, A.; Lehn, J.-M.; Eichen, Y. *J. Phys. Chem.* **1996**, *100*, 16175. (b) Casalegno, R.; Corval, A.; Kuldova, K.; Ziane, O.; Trommsdorff, H. P. *J. Lumin.* **1997**, *72*−*74*, 78. (c) Ziane, O.; Casalegno, R.; Corval, A. *Chem. Phys.* **1999**, *250*, 199. (d) Shinohara, S.; Takeda, J.; Ooike, T.; Kurita, S. *J. Phys. Soc. Jpn.* **1999**, *68*, 1725. (e) Schworer, M.; Wirz, J. *Helv. Chim. Acta* **2001**, *84*, 1441. (f) Corval, A.; Casalegno, R.; Ziane, O.; Burrows, H. D. *J. Phys. Chem. A* **2002**, *106*, 4272. (g) Naumov, P. *Bull. Chem. Technol. Macedonia* **2004**, *23*, 87. (i) Naumov, P. *J. Mol. Struct.* **2006**, *783*, 1.

(7) To the best of our knowledge, the only experimental report of a structure of the aci-nitro form determined with diffraction methods is that of the dinitrophenyl aci-nitro methane, where it is stabilized by a combination of electronic effects and exists as hydrogen bonded dimer: Bock, H.; Dieneli, R.; Schodel, H.; Havlas, Z,; Herdtweck, E.; Herrmann, W. A. *Angew Chem., Int. Ed.* **1993**, *32*, 1758. There is, however, a report on the silyl esters of the aci-nitro group: Colvin, E. W.; Beck, A. K.; Bastani, B.; Seebach, D.; Kai, Y.; Dunitz, J. D. *Helv. Chim. Acta* **2004**, *3*, 697.

(8) Foresman, J. B.; Head-Gordon, M.; Pople, J. A.; Frisch, J. M. *J. Phys. Chem.* **1992**, *96*, 135.

(9) Frisch, M. J.; Trucks, G. W.; Schlegel, H. B.; et al. *Gaussian03, Revision B.05*; Gaussian, Inc.: Wallingford CT, 2004 (the complete reference is provided in the Supporting Information).

(10) *APEX2 (ver. 2.1*−*4) and SAINT (ver. 7.34A)*. Bruker AXS, Inc.: Madison, WI, 2007.

(11) Sheldrick, G. M. *SADABS*; University of Göttingen: Göttingen, Germany, 1996.

(12) (a) Sheldrick, G. M. *Acta Crystallogr., Sect. A* **2008**, *64*, 112. (b) Altomare, A.; Cascarano, G.; Giacovazzo, C.; Guagliardi, A.; Burla, M. C.; Polidori, G.; Camalli, M. *J. Appl. Crystallogr.* **1994**, *27*, 435.

(13) Sheldrick, G. M. E. *SHELXL-97*; University of Göttingen: Göttingen, Germany, 1997.

(14) For details of the controlled heating device for single crystal X-ray diffraction see: Ishizawa, N., Kondo, S., Hibino, H., Igarashi, S., Nakamura, M., Saho, R. *Annual Report of the Ceramics Research Laboratory 2006*; Nagoya Institute of Technology: Gifu, Japan, 2007; Vol. 6, p 12. For a successful application see: Ishizawa, N.; Tateishi, K.; Kondo, S.; Suwa, T. *Inorg. Chem.* **2008**, *47*, 558.

(15) One of the hydroxyalkyl chains in form B BDB2 is disordered over two positions.

(16) The lowest singlet transition calculated with the CIS method on optimized BDB2 structure in a locked conformation (with intramolecular hydrogen bond between the terminal hydroxyl groups) and the respective oscillator strengths is at 389 nm. More accurate prediction of the absolute value should take into account multiple excitations.

(17) (a) Pogodin, S.; Rae, I. D.; Agranat, I. *Eur. J. Org. Chem.* **2006**, 5059. (b) Biedermann, P. U.; Stezowski, J. J.; Agranat, I. *Chem.—Eur. J.* **2006**, *12*, 3345. (c) Levy, A.; Pogodin, S.; Cohen, S.; Agranat, I. *Eur. J. Org. Chem.* **2007**, 5198. (d) Pogodin, S.; Suissa, M. R.; Levy, A.; Cohen, S.; Agranat, I. *Eur. J. Org. Chem.* **2008**, 2887.

(18) (a) Hadjoudis, E. In *Photochromism. Molecules and systems*; Dürr, H., Bouas-Laurent, H., Eds.; Elsevier: Amsterdam, 2003. (b) Sliwa, M.; Spangenberg, A.; Malfant, I.; Lacroix, P. G.; Metivier, R.; Pansu, R. B.; Nakatani, K. *Chem. Mater.* **2008**, *20*, 4062. (c) Harada, J.; Fujiwara, T.; Ogawa, K. *J. Am. Chem. Soc.* **2007**, *129*, 16216. (d) Fujiwara, T.; Harada, J.; Ogawa, K. *J. Phys. Chem. B* **2004**, *108*, 4035. (e) Plaquet, A.; Guillaume, M.; Champagne, B.; Rougier, L.; Mançois, F.; Rodriguez, V.; Pozzo, J.-L.; Ducasse, L.; Castet, F. *J. Phys. Chem. C* **2008**, *112*, 5638.

(19) Selected examples:(a) Tsuda, A.; Sakamoto, S.; Yamaguchi, K.; Aida, T. *J. Am. Chem. Soc.* **2003**, *125*, 15722. (b) Nishida, S.; Morita, Y.; Fukui, K.; Sato, K.; Shiomi, D.; Takui, T.; Nakasuji, K. *Angew. Chem., Int. Ed.* **2005**, *44*, 7277. (c) Morita, Y.; Suzuki, S.; Fukui, K.; Nakazawa, S.; Kitagawa, H.; Kishida, H.; Okamoto, H.; Naito, A.; Sekine, A.; Ohashi, Y.; Shiro, M.; Sasaki, K.; Shiomi, D.; Sato, K.; Takui, T.; Nakasuji, K. *Nat. Mater.* **2007**, *7*, 48. (d) Suzuki, S.; Morita, Y.; Fukui, K.; Sato, K.; Shiomi, D.; Takui, T.; Nakasuji, K. *J. Am. Chem. Soc.* **2006**, *128*, 2530.

(20) (a) Monkman, A. P.; Pålsson, L.-O.; Higgins, R. W. T.; Wang, C.; Bryce, M. R.; Batsanov, A. S.; Howard, J. A. K. *J. Am. Chem. Soc.* **2002**, *124*, 6049. (b) Wang, C.; Pålsson, L.-O.; Batsanov, A. S.; Bryce, M. R. *J. Am. Chem. Soc.* **2006**, *128*, 3789. (c) Bartholomew, G. P.; Bazan, G. C. *J. Am. Chem. Soc.* **2002**, *124*, 5183.

(21) (a) Blumstein, A.; Thomas, O. *Macromolecules* **1982**, *15*, 1264. (b) Abe, A. *Macromolecules* **1984**, *17*, 2280. (c) Domszy, R. C.; Shannon, P. J. *Macromolecules* **1990**, *23*, 2790. (d) Mather, P. T.; Jeon, H. G.; Han, C. D.; Chang, S. *Macromolecules* **2002**, *35*, 1326.

(22) (a) Bernstein, J. *Polymorphism in molecular crystals*; Oxford University Press: Oxford, 2002. (b) Anthony, A.; Desiraju, G. R.; Jetti, R. K. R.; Kuduva, S. S.; Madhavi, N. N. L.; Nangia, A.; Thaimattam, R.; Thalladi, V. R. *Mater. Res. Bull.* **1998**, *33*, 1. (c) Dunitz, J. D.; Gavezzotti, A. *Acc. Chem. Res.* **1999**, *32*, 677. (d) Bernstein, J.; Davey, R. J.; Henck, J. O. *Angew. Chem., Int. Ed.* **1999**, *38*, 3440. (e) Vishweshwar, P.; McMahon, J. A.; Oliveira, M.; Peterson, M. L.; Zaworotko, M. J. *J. Am. Chem. Soc.* **2005**, *127*, 16802. (f) Xu, M.; Harris, K. D. M. *J. Am. Chem. Soc.* **2005**, *127*, 10832. (g) Hiremath, R.; Basile, J. A.; Varney, S. W.; Swift, J. A. *J. Am. Chem. Soc.* **2005**, *127*, 18321. (h) Bernstein, J. *Chem. Commun.* **2005**, 5007. (i) Rafilovich, M; Bernstein, J. *J. Am. Chem. Soc.* **2006**, *128*, 12185. (j) Desgranges, C.; Delhommelle, J. *J. Am. Chem. Soc.* **2006**, *128*, 10368. (k) Ahn, S.; Guo, F.; Kariuki, B. M.; Harris, K. D. M. *J. Am. Chem. Soc.* **2006**, *128*, 8441. (l) Peterson, M. L.; Hickey, M. B.; Zaworotko, M. J.; Almarsson, O. *J. Pharm. Pharm. Sci.* **2006**, *9*, 317. (m) Reutzel-Edens, S. M. *Curr. Opin. Drug Discovery Dev.* **2006**, *9*, 806. (n) Curtis, D. M.; Nanos, J. I.; Moon, H.; Jahng, W. S. *J. Am. Chem. Soc.* **2007**, *129*, 15072. (o) Winkel, K.; Hage, W.; Loerting, T.; Price, S. L.; Mayer, E. *J. Am. Chem. Soc.* **2007**, *129*, 13863. (p) Zhang, T. H.; Liu, X. Y. *J. Am. Chem. Soc.* **2007**, *129*, 13520. (q) Beckham, G. T.; Peters, B.; Starbuck, C.; Variankaval, N.; Trout, B. L. *J. Am. Chem. Soc.* **2007**, *129*, 4714. (r) Hulme, A. T.; Johnston, A.; Florence, A. J.; Fernandes, P.; Shankland, K.; Bedford, C. T.; Welch, G. W. A.; Sadiq, G.; Haynes, D. A.; Motherwell, S. W. D.; Tocher, D. A; Price, S. L. *J. Am. Chem. Soc.* **2007**, *129*, 3649. (s) Das, D.; Barbour, L. J. *J. Am. Chem. Soc.* **2008**, *130*, 14032.

JP902517X